

Research Article

# Excess Heat from Palladium Deposited on Nickel

Tadahiko Mizuno\*

*Hydrogen Engineering Application and Development Company, Kita 12, Nishi 4, Kita-ku, Sapporo 001-0012, Japan*

Jed Rothwell†

*LENR-CANR.org, 1954 Airport Road, Suite 204, Chamblee, GA 30341, USA*

---

## Abstract

Two methods of generating excess heat with palladium on nickel are described: an older method, and a newer, faster method. With the older method after sufficient pretreatment, the output heat peaked at 232 W, which was nearly two times input power. However, the pretreatment was complicated and took many weeks or in some cases months before heat appeared. The newer method is to directly apply palladium to nickel. This is simpler and quicker, taking only about a day, but so far it has produced only 10–30 W, and 40 W in one instance.

© 2019 ISCMNS. All rights reserved. ISSN 2227-3123

**Keywords:** Air flow calorimetry, Deuterium gas, Excess heat, Nickel reactant, Pd coating, Simple method

---

## 1. Summary of Old Results

### 1.1. Old method

A reactor with a cruciform shape was first used in this project (Fig. 1). It weighs 50 kg. Later, 20-kg versions of this reactor were used, as well as cylindrical reactors. All have palladium rods in the center. The rods are 250 mm long, wound with palladium wire (Fig. 2). This is the positive electrode. The negative electrode is a nickel mesh which is fitted against the inside wall of the reactor, and connected to ground (Fig. 3).

The older method is described in detail elsewhere [1]. It includes several rounds of cleaning the electrodes by heating and evacuation to remove impurities, followed by weeks or months of glow discharge to erode the center palladium electrode and sputter palladium onto the nickel mesh.

The highest power observed with the older method was 480 W output with 248 W input, or 232 W excess (Fig. 4). In this example, heating was stopped at 83 ks and the reaction stopped, but when heating is continued, excess heat

---

\*Corresponding author. E-mail: head-mizuno@lake.ocn.ne.jp.

†E-mail: JedRothwell@gmail.com.

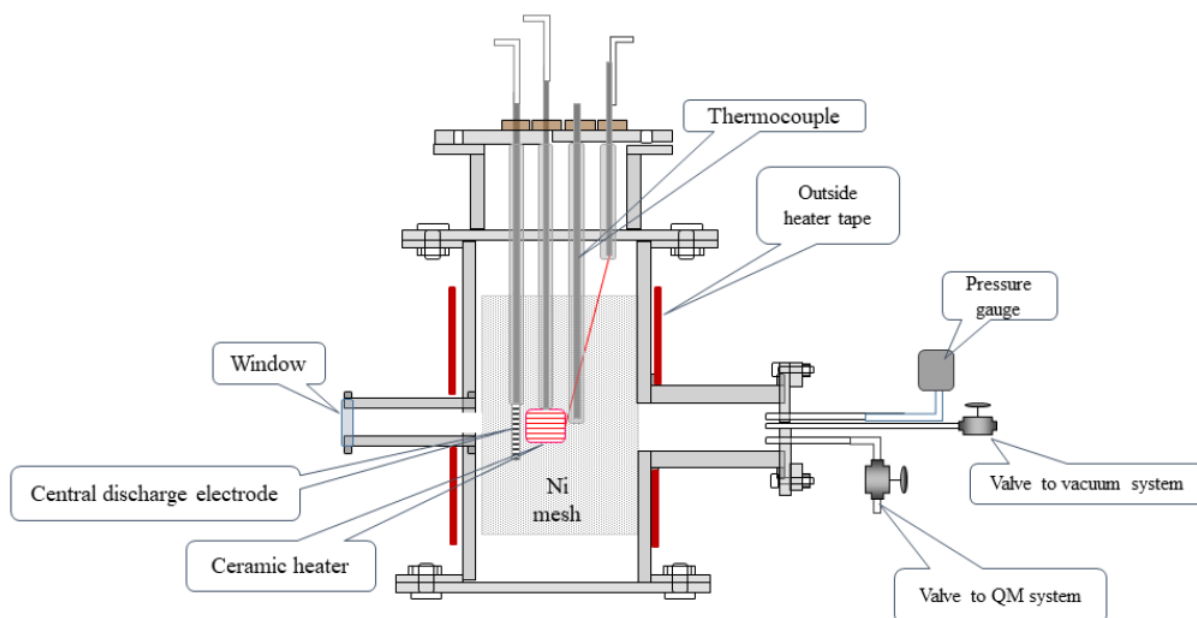


**Figure 1.** Schematic of the old cruciform reactor (height 500 mm, diameter 213 mm, volume 5.53 L, weight 50.5 kg) A pair of 20 kg versions were used with the new method, one for control, and one for the active cell. The cell contains a central discharge electrode, nickel mesh electrode, and a ceramic heater with palladium wire wound around it.

generation also continues. Unfortunately, this method sometimes took months to turn on. This long delay tied up equipment and hampered the research.

### 1.2. Old electrode preparation method

Here are the electrode activation procedures for a mesh of 50–100 g as follows.

- (1) Place the electrodes in the reactor. The reactant metal is degassed initially at room temperature. This is to avoid the formation of an oxide film or nitride film that would be strengthened by the in-system gas when it is processed at high temperature, so that the subsequent activation treatment becomes difficult.



**Figure 2.** Central discharge electrode. A 250 mm palladium rod, wound with palladium wire.

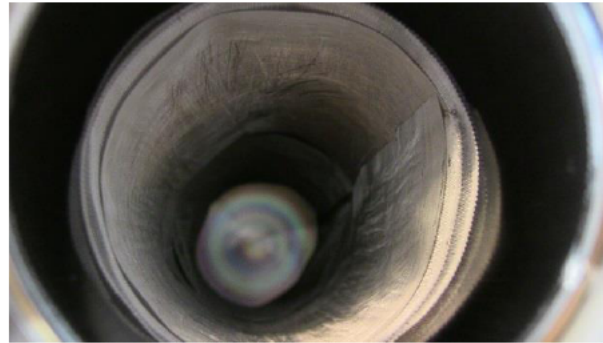


**Figure 3.** Mesh electrode mounted inside the reactor placed against the reactor wall, connected to ground.

- (2) Heat in vacuum to remove the impurity gases generated in the metal film formation process. It is important to begin heating after sufficient removal of impurities at low temperatures (step 1). The reactor gas should be checked with a mass spectrometer each time heating in vacuum is repeated, to confirm that contamination is decreasing. When the reactor is not sufficiently exhausted,  $\text{H}_2\text{O}$ , nitrogen and oxygen gases will remain in it. In a Q-Mass observation, component peaks of  $\text{H}_2\text{O}$  (16,17, and 18) should be lower than the ionic current value of  $10^{-9}$  A.
  - (3) After the temperature measured on the reactor wall at mid-height reaches  $200^\circ\text{C}$ , and the reactor is at uniform temperature,  $\text{D}_2$  gas is introduced at 50 Pa. If the mesh was previously used in experiments, and it was sputtered with palladium from glow discharge, it should be successfully re-activated, and excess heat will be generated immediately. If not, steps 2 and 3 may need to be repeated several times.
  - (4) An unused mesh has to be exposed to glow discharge over many days or weeks, and sputtered with palladium.
- After these steps, gas pressure in the reactor is set at 200–1000 Pa. Deuterium absorption/desorption treatment on

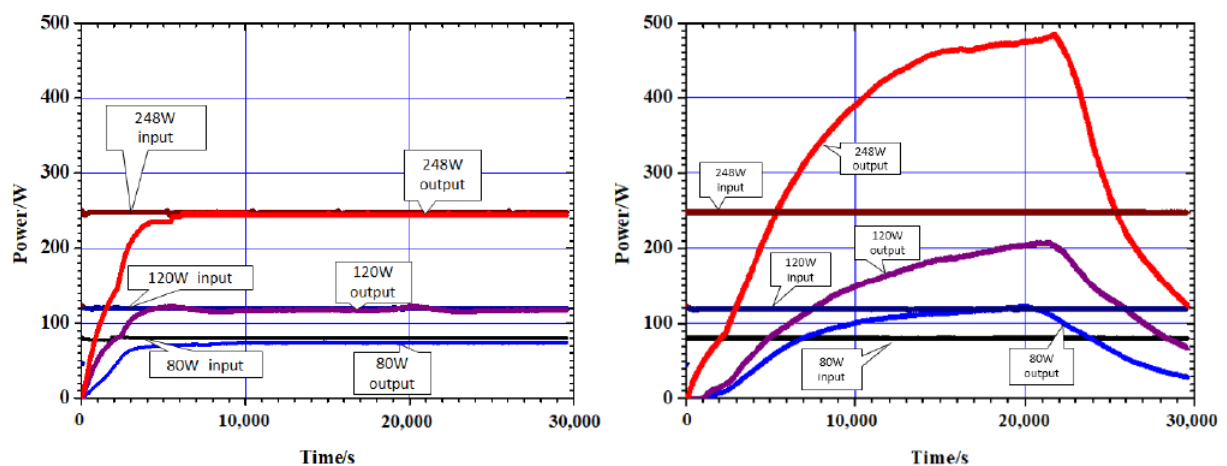


**Figure 4.** Old results – (Left) Calibrations at various power levels. (Right) Excess heat at the same power levels.

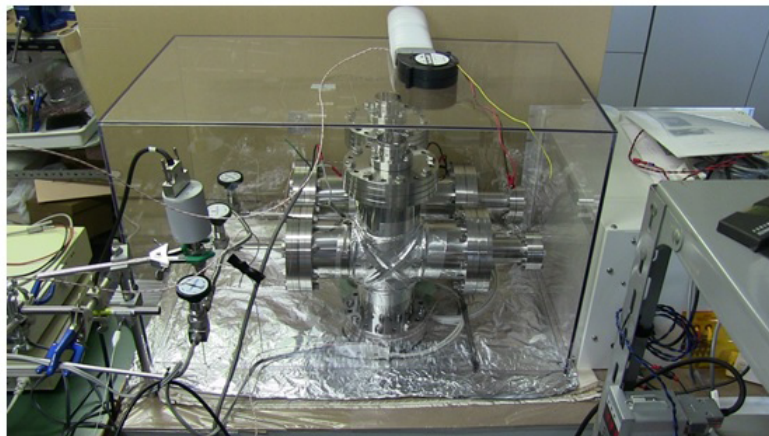


**Figure 5.** The calorimeter acrylic box, with the insulation removed to show the equipment placed inside. The active and control reactors are side-by-side in box. These are the 20-kg cruciform reactors.



**Figure 6.** Cylindrical reactors. Length 500 mm, diameter 120 mm, weight 20 kg. A cylindrical reactor and a control reactor (*in red box*) are placed side-by-side in the calorimeter.

the reactant metal surface causes hydrogen embrittlement to atomize the surface metal. This method is to raise the temperature of the reactor wall from room temperature to 300°C, and repeatedly cool it.

The heating time is 10–15 h and the cooling time is 4–6 h, that is, about one cycle per day. This process should

be repeated as many times as possible, but as a practical matter it is usually repeated about 5–6 times. This process is essential for large excess heat generation.

Excess heat is governed by gas pressure, reactant weight, and input power. When excess heat is generated, the temperature of the reactant increases by several tens of degrees. The reactant is the nickel mesh that is thinly covered with Pd. The temperature of the nickel mesh cannot be measured directly.

As the reactant temperature rises, the amount of deuterium in the reactant decreases. This causes the exothermic reaction to decrease and the reactant temperature to fall. When the temperature decreases, more deuterium enters the reactant again, and excess heat increases.

### 1.3. Heat apparently produced by mesh

The nickel mesh apparently produces excess heat, presumably because it was gradually sputtered with palladium nanoparticles during the preparation and subsequent glow discharge. The mesh appears to be where the excess heat reaction occurs, rather than the central palladium rod electrode. Evidence for this includes:

- (1) The reaction increases when the reactor vessel itself is heated from the outside. This affects the nickel mesh more than other components.
- (2) The reaction can be reliably triggered with palladium deposited on the mesh, with the newer method.

At a power density of 10 W/g, in principle the maximum temperature might reach  $\sim 1000^{\circ}\text{C}$ , depending on the heat resistance and heat losses of the reactor. A temperature apparently as high as  $850^{\circ}\text{C}$  has already been reached.

The temperature is determined by the amount of reactant and the removal rate of heat. In principle, a high temperature can be obtained at any rate, by increasing the insulation of the calorimeter.

### 1.4. Old method of calorimetry

In the beginning of this project, isoperibolic calorimetry was used. In this method, water was circulated through tubes wrapped around the reactor, and the entire reactor was set to a uniform temperature. Thermal calculation accurately

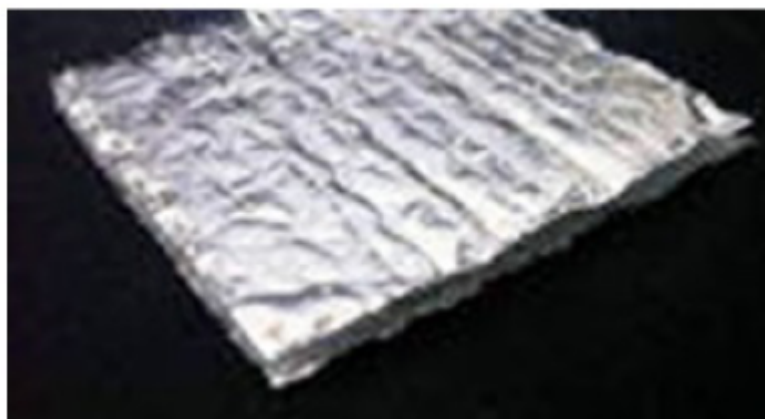


**Figure 7.** A layer of this reflective padded aluminum insulation is placed on the inside of the box reducing heat leaks to a minimum. At 100–200 W, the inside of the box is only moderately hotter than the surroundings at  $\sim 36^{\circ}\text{C}$ , so only  $\sim 4\%$  of the heat is lost through the walls and insulation. The rest is recovered in the flowing air.

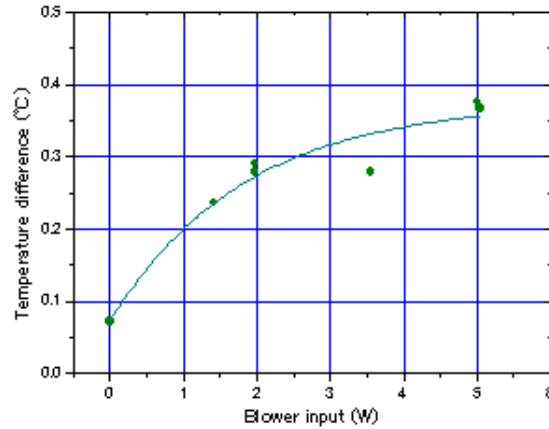


**Figure 8.** Calibration with blower power only, and no power to the reactors. The temperature rise of  $\sim 3.5^\circ\text{C}$  is probably caused by waste heat from the blower motor reaching the outlet RTDs.

measured the heat transfer between three systems: the surrounding environment, the reactor body, and the circulation pump reservoir. This method was repeatedly tested with calibrations and exothermic tests to statistically verify the difference between both tests. Significant excess heat was confirmed by Welch's test [2]. However, although this method of calculating excess heat generation is in principle correct, it was complicated, so it was replaced with airflow calorimetry. Airflow calorimetry is more direct, easier to understand, and it allows the reactor body to reach a higher temperature. It is described in Section 2.

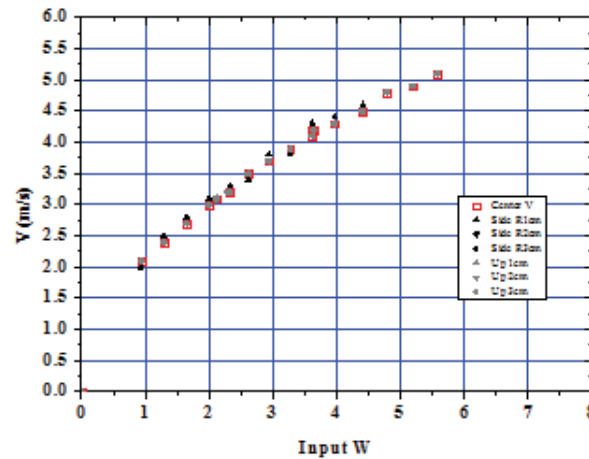


**Figure 9.** Relationship between blower power and air velocity at the outlet for different locations of the anemometer across the tube section. The velocity profile is almost uniform.

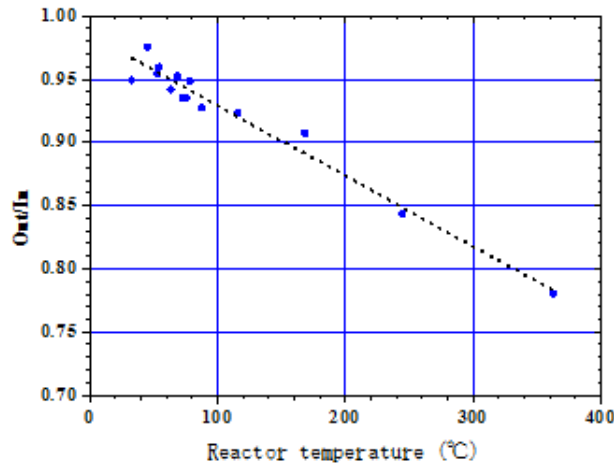


Figure 10. Calibration reactor temperature and heat recovery rate.

## 2. New Method

### 2.1. Newer, simplified method of preparing mesh

The newer method is to directly apply palladium to the nickel mesh, either by rubbing a palladium rod onto the mesh, or by electroless plating, rather than waiting for glow discharge to gradually sputter the palladium onto the mesh. This is simpler and quicker, taking only about a day, but so far it has only produced 10–30 W, or 5–15% of input power, and up to 40 W in one instance.

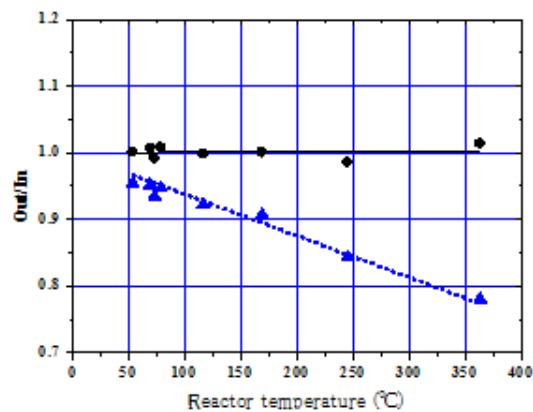


Figure 11. Thermal calibration with and without including heat recovery.

**Table 1.** Ni mesh surface rubbed with Pd rod

Reactor type	Y/M/D	Gas	Pressure (Pa)	Input (W)	Input (MJ)	Output (MJ)	Out/In ratio
Horizontal reactor	2017-07-31	H <sub>2</sub>	1000	100	1.68	1.85	1.10
Cruciform reactor	2017-08-11	H <sub>2</sub>	1000	100	1.99	1.99	1.00
<b>Control reactor</b>	<b>2017-08-11</b>			<b>100</b>	<b>0.95</b>	<b>0.95</b>	<b>1.00</b>
Small reactor	2017-08-16	D <sub>2</sub>	4300	100	1.13	1.31	1.16
<b>Control reactor</b>	<b>2017-08-17</b>			<b>100</b>	<b>1.10</b>	<b>1.05</b>	<b>0.96</b>
Horizontal reactor	2017-08-22	H <sub>2</sub>	4400	100	2.48	2.65	1.07
<b>Control reactor</b>	<b>2017-08-23</b>			<b>100</b>	<b>1.07</b>	<b>1.05</b>	<b>0.98</b>
<b>Control reactor</b>	<b>2017-08-24</b>			<b>100</b>	<b>0.72</b>	<b>0.70</b>	<b>0.96</b>
Cruciform reactor	2017-09-03	D <sub>2</sub>	5	100	0.87	1.08	1.24
Cruciform reactor	2017-09-04	D <sub>2</sub>	440	100	2.02	2.18	1.08
Cruciform reactor	2017-09-05	D <sub>2</sub>	440	100	4.68	4.73	1.01
Cruciform reactor	2017-09-06	D <sub>2</sub>	450	100	2.22	2.49	1.12
<b>Control reactor</b>	<b>2017-09-22</b>			<b>100</b>	<b>7.13</b>	<b>7.13</b>	<b>1.00</b>
<b>Control reactor</b>	<b>2017-10-24</b>			<b>100</b>	<b>5.95</b>	<b>5.95</b>	<b>1.00</b>
Cruciform reactor	2017-10-25	D <sub>2</sub>	700	100	6.95	6.97	1.00
Cruciform reactor	2017-10-30	D <sub>2</sub>	700	100	8.49	8.57	1.01
Cruciform reactor	2017-11-04	D <sub>2</sub>	450	200	35.01	34.39	0.98
Cruciform reactor	2017-11-06	D <sub>2</sub>	450	200	34.87	34.42	0.99
Cruciform reactor	2017-11-11	D <sub>2</sub>	450	100	9.27	9.35	1.01
Cruciform reactor	2017-11-14	D <sub>2</sub>	450	400	5.20	5.54	1.07
<b>Control reactor</b>	<b>2017-11-15</b>			<b>400</b>	<b>5.19</b>	<b>5.12</b>	<b>0.99</b>
Cruciform reactor	2017-11-16	D <sub>2</sub>	450	400	8.70	9.16	1.05
Cruciform reactor	2016-11-17	D <sub>2</sub>	450	200	4.79	5.21	1.09
Cruciform reactor	2017-11-20	D <sub>2</sub>	1000	200	17.18	18.40	1.07
Cruciform reactor	2017-11-21	D <sub>2</sub>	750	200	12.28	13.30	1.08
<b>Control reactor</b>	<b>2017-11-22</b>			<b>200</b>	<b>31.02</b>	<b>31.03</b>	<b>1.00</b>
<b>Control reactor</b>	<b>2017-11-24</b>			<b>200</b>	<b>7.86</b>	<b>7.84</b>	<b>1.00</b>
Cruciform reactor	2017-11-25	D <sub>2</sub>	750	100	15.80	16.98	1.08

Note: Rows in bold face are calibration tests.

All of the tests with the new method used airflow calorimetry. Two different pairs of reactors were used. The first pair were cruciform reactors similar to the one used with the older method, but smaller and lighter, weighing 20 kg instead of 50 kg. They are shown in Fig. 5 placed side-by-side in the calorimeter. The second pair were horizontal pipes (Fig. 6).

The electrode configuration was the same as with the old method, with a central rod electrode, and a mesh electrode placed against the reactor wall and connected to ground. The reaction gas was usually deuterium.

## 2.2. Airflow calorimetry

An insulated acrylic box is used for airflow calorimetry. It is 400 mm × 750 mm, height 700 mm. During a test, the inside of the plastic box is covered with 1.91 m<sup>2</sup> of reflective padded aluminum insulation (shanetsu.com, Fig. 7). This minimizes losses to radiation. These losses are low in any case, because the cooling air keeps the inside of the box at ~36°C (16°C above ambient). Similar insulation from a US vendor (US Energy Products) has an *R*-value of 11, so the insulation radiates ~3 W (16°C/11 W/m<sup>2</sup> × 1.9 m<sup>2</sup>). The air inlet and outlets are circular, 50 mm in diameter. The inlet is located near the bottom of one side, and the outlet is on the top surface. The outlet is connected to a pipe, which makes the airflow more uniform across all parts of the cross section of the outlet, to increase the accuracy of the airflow measurement. The power to the blower is continuously monitored.

The blower is operated at 6.5 W. The outlet air temperature is measured with two RTDs. They are installed in the



**Table 2.** Nickel mesh with Pd deposited by electroless plating

Reactor type	Y/M/D	Gas	Pressure/Pa	Input/W	Input/MJ	Output/MJ	Out/In ratio
Horizontal reactor	2018-02-07	D <sub>2</sub>	730	100	8.36	9.80	1.17
Horizontal reactor	2018-02-09	D <sub>2</sub>	730	200	4.83	5.52	1.14
Horizontal reactor	2018-02-11	D <sub>2</sub>	670	200	34.74	40.14	1.16
Horizontal reactor	2018-02-19	D <sub>2</sub>	670	200	16.38	17.94	1.10
Horizontal reactor	2018-02-21	D <sub>2</sub>	670	200	17.66	19.43	1.10
Horizontal reactor	2018-02-23	D <sub>2</sub>	670	200	19.99	20.30	1.02
Horizontal reactor	2018-02-26	D <sub>2</sub>	670	200	24.71	27.65	1.12
Horizontal reactor	2018-02-27	D <sub>2</sub>	670	200	34.05	38.51	1.13
<b>Control reactor</b>	<b>2018-03-02</b>			<b>200</b>	<b>12.02</b>	<b>12.01</b>	<b>1.00</b>
<b>Control reactor</b>	<b>2018-03-03</b>			<b>200</b>	<b>40.06</b>	<b>39.53</b>	<b>0.99</b>
Horizontal reactor	2018-03-06			500	9.49	9.23	0.97
<b>Control reactor</b>	<b>2018-03-07</b>			<b>500</b>	<b>11.77</b>	<b>10.53</b>	<b>0.89</b>
Horizontal reactor	2018-03-16	D <sub>2</sub>	670	200	12.65	14.49	1.15
Horizontal reactor	2018-03-29	D <sub>2</sub>	670	200	6.94	7.57	1.09
Horizontal reactor	2018-04-04	D <sub>2</sub>	590	200	14.99	17.09	1.14
<b>Control reactor</b>	<b>2018-04-05</b>			<b>200</b>	<b>6.44</b>	<b>6.44</b>	<b>1.00</b>
Horizontal reactor	2018-04-11	D <sub>2</sub>	310	200	3.62	3.89	1.08
Horizontal reactor	2018-04-13	D <sub>2</sub>	590	200	10.04	10.67	1.06
<b>Control reactor</b>	<b>2018-04-16</b>			<b>200</b>	<b>12.10</b>	<b>12.13</b>	<b>1.00</b>
Horizontal reactor	2018-04-20	D <sub>2</sub>	490	200	11.93	12.57	1.05
<b>Control reactor</b>	<b>2018-05-16</b>			<b>100</b>	<b>4.06</b>	<b>4.06</b>	<b>1.00</b>
Horizontal reactor	2018-05-16	D <sub>2</sub>	500	100	5.06	5.37	1.06
Horizontal reactor	2018-05-18	D <sub>2</sub> :500+H <sub>2</sub> :6000	6500	100	7.05	7.53	1.07
<b>Control reactor</b>	<b>2018-05-21</b>			<b>100</b>	<b>5.45</b>	<b>5.45</b>	<b>1.00</b>
<b>Control reactor</b>	<b>2018-05-23</b>			<b>0</b>	<b>4</b>	<b>-1,547</b>	
Horizontal reactor	2018-05-23	D <sub>2</sub> :500+H <sub>2</sub> :6000	6500	200	8.04	8.42	1.05
Horizontal reactor	2018-05-25	D <sub>2</sub> :500+H <sub>2</sub> :6000	6500	200	14.03	14.18	1.01

Note: Rows in bold face are calibration tests.

center of the pipe, one in the stream of air before it reaches the blower, and one after it, to measure any heat added to the stream of air by the blower motor. The difference between the two is less than 0.1°C. However, there are indications that heat from the blower motor is affecting both of them. A calibration with no input power to the reactors shows that when the blower power is stepped from 1.5 to 5 W, the outlet RTDs are ~0.35°C warmer than inlet (Fig. 8). This is a much larger temperature difference than the moving air in the box alone could produce.

Blowers are inefficient, so most of the input power to the blower converts to waste heat in the motor. It seems likely some of this heat is conducted by the pipe to raise the temperature of the two outlet RTDs.

The airflow rate is measured with a hot wire digital anemometer (CW-60, Custom Co. Ltd.). The flow of air through the box is confirmed by letting smoke from incense into the box, and then timing how long it takes for all of the smoke to clear out.

The air velocity profile across the tube section was checked by placing the hot wire at different locations along two perpendicular diameters. The results are displayed in Fig. 9. The distribution is fairly uniform so that the average air velocity across the tube is well characterized by the velocity measured on the axis.

With the new method, a pair of reactors are installed in the air flow box: an active cell and a control cell. They are placed on insulating bricks to reduce heat losses through the table. They are the same size and design. One is active and the other is the calibration control. The control reactor is kept at the same pressure and input power as the active reactor. The two are periodically swapped. The control becomes the active reactor. The calorimeter is not opened while a series of control and active tests are performed, so conditions in it remain closely similar for both tests.

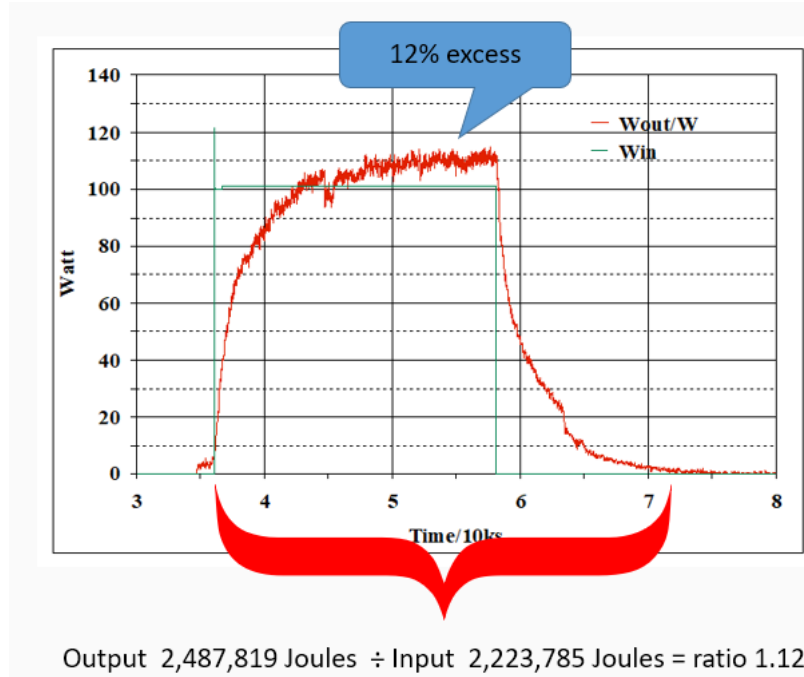


**Figure 12.** An example of 12% excess heat. Both input and output energy are measured from turn on to cool down.

Two kinds of control tests are done. In the first, the control reactor is heated at the outer wall heater. In the second, glow discharge using ordinary electrodes and hydrogen was performed. Both methods show no excess heat.

In the first approximation, the airflow calorimetry is simple. The number of liters of air that pass through the box per second is computed, based on the size of the duct and the speed of the air leaving the duct. The temperature difference between the inlet and the outlet is measured. Energy is computed as follows:

$$E_{\text{out}} = V \rho C_p \Delta T, \quad (1)$$

where  $E_{\text{out}}$  is the output energy captured by the airflow ( $\text{Js}^{-1}$ ),  $V$  the volumetric air flow rate ( $\text{m}^3\text{s}^{-1}$ ),  $\rho$  the density of air at the outlet temperature ( $\text{kgm}^{-3}$ ),  $C_p$  the heat capacity of air at constant pressure ( $\text{Jkg}^{-1}\text{K}^{-1}$ ) and  $\Delta T$  is the temperature difference between the air box inlet and outlet (K).

The air density is calculated for the temperature at the outlet where the velocity is measured. The variation of the atmospheric pressure is not taken into account because its influence is small. The heat losses of the air box were evaluated. The heat losses increase with the energy input that influences the temperature difference between the air inlet and outlet as well as the reactor wall temperature. The ratio of the heat captured by the airflow to the energy input is called the heat recovery rate.

Figure 10 shows the reactor temperature vs. the heat recovery rate. When there is no input power, and the reactor body temperature is  $25^\circ\text{C}$ , the recovery rate should be close to 1. When the reactor body temperature is  $100^\circ\text{C}$ , the recovery rate is 0.93; it is 0.82 at  $300^\circ\text{C}$ , and 0.78 at  $360^\circ\text{C}$ . Naturally this is the same in the test reactor as the calibration reactor; the recovery rate decreases as the temperature of the test reactor rises. The approximate expression showing this ratio is the linear approximation:

$$O/I = 0.98 - 5.0811 \times 10^{-4} \times t, \quad (2)$$

where  $t$  is the reactor temperature ( $^{\circ}\text{C}$ ).

When the calibration data is recalculated taking into account the heat recovery rates in Fig. 10, the results shown in Fig. 11 are obtained. In this graph, the temperature of the calibration reactor is plotted on the horizontal axis and the output/input ratio is plotted on the vertical axis. In Fig. 11, the marks do not include the heat recovery rate calibration, and the  $\cdot$  marks show the data after taking into account the heat recovery rate. If the temperature rise during the calibration of the reactor is computed without taking into account heat recovery the  $O/I$  ratio = 0.78 at  $363^{\circ}\text{C}$  for example. These values are extremely close to  $O/I = 1$  after the heat recovery correction according to Eq. (2).

Six parameters (reactor temperatures, air inlet and outlet temperatures, input current and voltage, and blower power) were recorded every 5 s in spreadsheets. The power for each 5-second interval is computed. The record begins when power is turned on. After the power is turned off, the data continues to be recorded until the temperature falls back to room temperature. The total input and output energy for this entire period is added up, and the ratio is computed. Figure 12 shows an example with 12% excess heat.

### 2.3. Activation process with new method

Palladium is first applied to the nickel screen. This has been done with two methods. The first is to rub the nickel screen with a palladium rod. The second is to deposit a palladium film on the nickel mesh surface by plating it with an electroless plating solution of palladium of Pd-10 (High Purity Chemical Co. Ltd.), Pd concentration 10 g/L. The plating conditions are:  $40\text{--}60^{\circ}\text{C}$ , pH 1.5.

The preparation steps are as follows.

- (1) Wash with a mild detergent in ordinary tap water, and scrub with a plastic dish washing pad.
- (2) Sand with water resistant sandpaper, starting with 250 grit, then 400, then 1000. Wash with mild detergent and rinse with tap water.

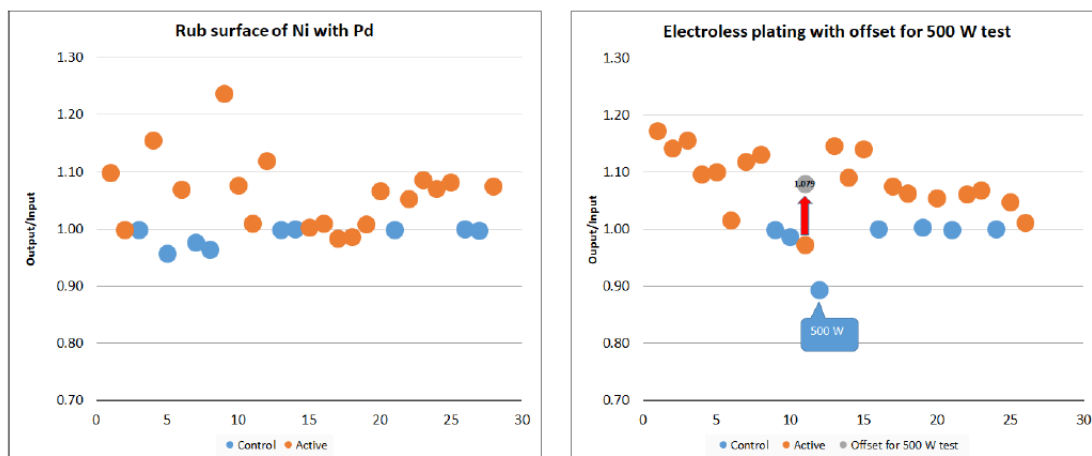


**Figure 13.** (Left) Nickel rubbed with palladium. (Right) Electroless plating. The 500 W active test is adjusted to the recovery rate shown by the 500 W calibration (grey dot).

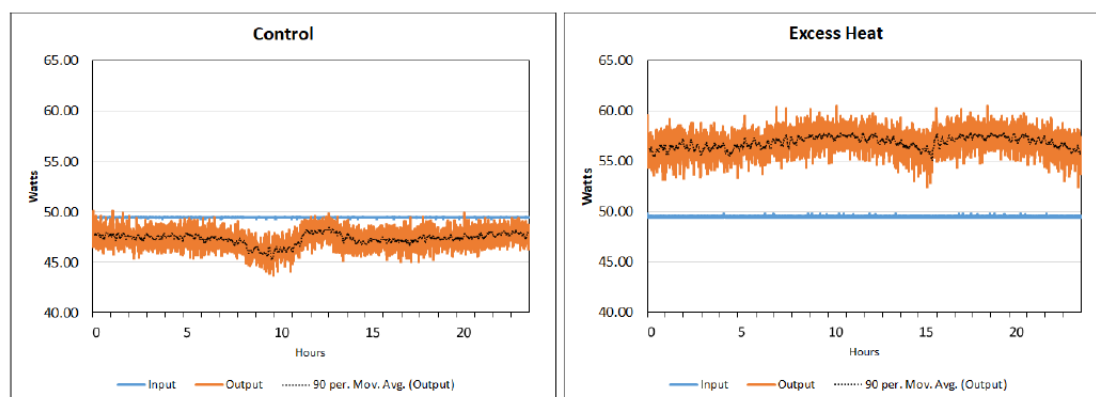


**Figure 14.** Recent results. 24-hour samples of: (left) Control test (2018–08–08) and (right) Excess heat test (2018–08–20).

- (3) Soak in tap water at about 90°C for a while.
- (4) Wash with alcohol.

This process removes oil and roughens the metal surface. After cleaning:

- (1) The mesh is placed in reactor. Gas discharge, vacuum evacuation to  $10^{-2}$  Pa at room temperature for about 2 h.
- (2) Heat treatment, in which pretreatment (removal of impurities and surface refinement) of the reactant metal surface is carried out. The temperature is 100–120°C duration 5–20 h.
- (3) Mesh is removed from reactor. At this stage the surface should be free of contaminants. Coating of palladium on nickel, with rubbing or electroless deposition plating.
- (4) Mesh is placed in reactor again. Heated for 1–2 h.
- (5) Cool down in the reactor, 1–2 h.

Steps 4 and 5 may need to be repeated a few times.

Although this method is simple and fast compared to the old method, excess heat is generally 10 W, up to 40 W in one instance, and the output/input ratio is small. Tables 1 and 2 and the graphs in Fig. 13 shows the test results of palladium adhered to the nickel mesh by rubbing and electroless plating. Figure 14 shows the results of a particular test as an example.

### 3. Summary

The previous method was effective for generating excess heat. In the best case, this method generated several hundred watts of excess heat. The reaction sometimes continued for several months. However, the process of fabricating and then activating the nano-particles was complicated and cumbersome, and it took a long time. With the new method of applying palladium to the nickel surface, excess heat is more likely to occur. This method is simpler and much faster. However, the excess is usually only 5–6% of the input power, and the best results so far were ~20% (10–40 W). The future goal is to investigate higher temperature excess heat and reactants.

## References

- [1] T. Mizuno, Observation of excess heat by activated metal and deuterium gas, *J. Condensed Matter Nucl. Sci.* **25** (2017) 1–25.
- [2] T. Mizuno and H Yoshino, Confirmation of excess heat generation during metal–hydrogen reaction, *Proc. JCF16*, Kyoto, Japan, Dec. 11–15, 2015, pp. 16–27.